ELSEVIER

Physics of the Earth and Planetary Interiors 117 (2000) 123–137

PHYSICS OF THE EARTH AND PLANETARY INTERIORS

www.elsevier.com/locate/pepi

Ab initio free energy calculations on the polymorphs of iron at core conditions

Lidunka Vočadlo [a,*], John Brodholt [a], Dario Alfè [a], Michael J. Gillan [b], Geoffrey D. Price [a]

[a] *Research School of Geological and Geophysical Sciences, Birkbeck College and University College London, Gower Street, London, WC1E 6BT, UK*

[b] *Department of Physics and Astronomy, University College London, Gower Street, London, WC1E 6BT, UK*

Received 3 November 1998; accepted 17 May 1999

Abstract

In order to predict the stable polymorph of iron under core conditions, calculations have been performed on all the candidate phases proposed for inner core conditions, namely, body-centred cubic (bcc), body-centred tetragonal (bct), hexagonal close-packed (hcp), double-hexagonal close-packed (dhcp) and an orthorhombically distorted hcp polymorph. Our simulations are ab initio free energy electronic structure calculations, based upon density functional theory, within the generalised gradient approximation; we use Vanderbilt ultrasoft non-normconserving pseudopotentials to describe the core interactions, and the frozen phonon technique to obtain the vibrational characteristics of the candidate structures. Our results show that under conditions of hydrostatic stress, the orthorhombic, bcc and bct structures are mechanically unstable. The relative free energies of the remaining phases indicate that dhcp and fcc Fe are thermodynamically less stable than hcp Fe, therefore, we predict that the stable phase of iron at core conditions is hcp-Fe.

Keywords: Core conditions; Iron; Polymorphs

1. Introduction

The inferred density of the Earth's inner core suggests that it is made predominantly of iron with some lighter alloying elements. In order to understand the inner core and interpret the observed seismic anisotropy, we would ideally like to have information on all multiphase systems containing iron and candidate lighter elements at core conditions. However, even the high pressure (P), high temperature (T) phase diagram of pure iron presents major problems, which must be resolved before the more complex phases can be properly understood. Direct observation of the high P/T behaviour of iron is extremely difficult, with experimental groups getting conflicting results. In particular, the possibility of a solid–solid phase transition from hexagonal close-packed (hcp) to a structurally ill-defined β-phase has been observed above ~ 35 GPa and ~ 1500 K through in situ X-ray diffraction (XRD) experiments

* Corresponding author. E-mail: l.vocadlo@ucl.ac.uk

0031-9201/00/$ - see front matter
PII: S0031-9201(99)00092-8

(Boehler, 1993; Saxena et al., 1996; Andrault et al., 1997). It has been suggested that the crystal structure of this phase could be double-hexagonal close-packed dhcp-Fe (Saxena et al., 1996) or an orthorhombically distorted hcp polymorph (Andrault et al., 1997). However, more recent in situ XRD experiments by another group have observed no such phase transition (Shen et al., 1998) with hcp-Fe remaining stable at high P and T until the onset of melting. Moreover, the existence of another solid–solid phase boundary above $\sim$200 GPa and $\sim$4000 K has been suggested to reconcile data from static and shock experiments (Anderson and Duba, 1997) (Fig. 1). Although the structure of this phase is unknown, it has been suggested that it might be body-centred cubic (bcc)-Fe (Bassett and Weathers, 1990); this is supported by classical molecular dynamics calculations (Matsui, 1993), but the results of such calculations are hampered by the validity of using parameterised potentials beyond the range of their empirical fitting. More recently, however, the very latest shock experiments (Nguyen and Holmes, 1998) indicate that hcp-Fe remains stable at very high P/T undergoing no such phase change, in contrast to the earlier results of Brown and McQueen (1986).

The uncertainties in the iron phase diagram can be resolved in principle by using ab initio calculations, which provide an accurate means of calculating the thermoelastic properties of materials at high P and T by solving from first principles for the electronic structure of the system of interest. High pressure phases of iron have been studied extensively and successfully using a number of first principles techniques (e.g., Stixrude et al., 1994; Stixrude and Cohen, 1995; Södelind et al., 1996; Vočadlo et al., 1997). However, high P and T calculations on iron are significantly more difficult since they require substantially more computer resources. Using ab initio calculations to parameterise a tight-binding model, Wasserman et al. (1996) and Stixrude et al. (1997) have modelled both fcc and hcp-Fe at core P and T. By using a statistical mechanical scheme, they were

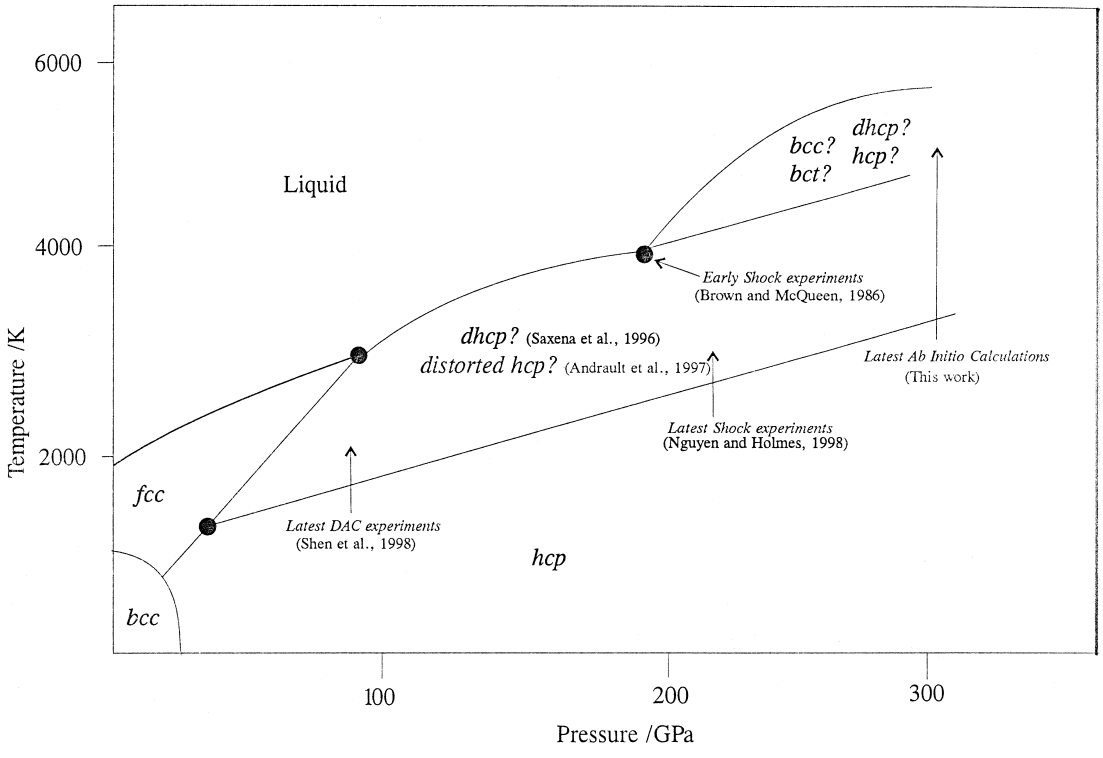

Fig. 1. The phase diagram of iron which shows the experimentally inferred solid–solid phase transformations to high P/T polymorphs of unknown structure.

able to obtain a number of thermodynamic properties at high P and T for these two phases. However, they did not consider the dhcp or orthorhombic phase.

In contrast to this previous work, in this paper, we present fully ab initio calculations on all the candidate structures of iron, performed on the Cray T3E at Edinburgh, in order to determine their relative free energies, and therefore, the stable phase of iron at core conditions. We have used density functional theory (DFT) and the pseudopotential methodology for calculating the energy of the perfect lattice, and the frozen phonon technique for obtaining the vibrational characteristics of the phases at high temperatures.

In Section 2, we describe the methodology used in our pseudopotential calculations and describe the way in which we obtain the free energies. We then present the results of these simulations and show how they lead to relative free energy curves, which determine the stable structure at core conditions. Finally, we discuss the validity of our technique and the possible sources of uncertainty.

2. Simulation techniques for calculating free energies

2.1. Density functional theory and the pseudopotential method

In first principles simulations, the solid is represented as a collection of electrons and atomic nuclei, and ideally, we would like to calculate the energy and forces on every ion as a function of atomic position by solving Schrödinger's equation explicitly. However, this is impracticable, if not impossible, and the formidable task is made more feasible by the use of DFT. In DFT, an approximation is made for the electronic exchange and correlation; each electron is treated as a single particle wavefunction with the interaction between them represented by an effective potential. DFT can be applied either through all-electron calculations, in which the full electronic structure of the system is calculated, or through the use of pseudopotentials, in which only the valence electrons are treated explicitly, with the interaction between these and the ionic cores being represented by an ab initio pseudopotential. In both cases, the accuracy with which the material is described is governed by the approximation used for the exchange-correlation energy. The pseudopotential approach can be as accurate as all-electron methods but is computationally much less demanding (see, for example, Vočadlo et al., 1997). The simulations presented have been carried out using DFT, with the exchange-correlation energy being treated by the generalised gradient approximation (GGA) (Perdew et al., 1992). We have used Vanderbilt non-normconserving ultrasoft pseudopotentials (Vanderbilt, 1990) as implemented in the VASP code (Vienna ab initio simulation package, Kresse and Furthmüller, 1996). Details of the construction of the pseudopotentials can be found in Kresse and Hafner (1994), and specific information about iron pseudopotentials can be found in Moroni et al. (1997). The non-normconserving condition of these pseudopotentials allows the wavefunction of the pseudoatom and exact atom at some specified radius to be different; the advantage of this is that it allows the pseudowavefunction to be significantly smoother, and therefore, the number of coefficients required to describe the pseudowavefunction are reduced, making the calculations more efficient yet maintaining high accuracy. Another advantage of using these pseudopotentials is that it is possible to describe lower lying core states as valence states. This is very important in calculations on iron since we have previously found that in order to accurately model the properties of solid iron, it is essential to treat the $3p$ states as valence states with a [Ne]$3s^3$ core (Vočadlo et al., 1997).

The quality of our chosen pseudopotential has been reported previously (Vočadlo et al., 1997), where we found very good agreement with both all-electron calculations (Stixrude et al., 1994; Södelind et al., 1996) and experiment (Mao et al., 1990) for the density variation as a function of pressure for hcp-Fe to core pressures (Fig. 2). We also accurately reproduced the magnetic and elastic behaviour of bcc-Fe and the bcc $\rightarrow$ hcp phase transition (a magnetic moment of 2.25 μ/atom compared with the experimental value of 2.12 μ/atom, an incompressibility, K, of 184 GPa compared to the experimental value of 173 GPa, and a transition pressure of $\sim$ 10

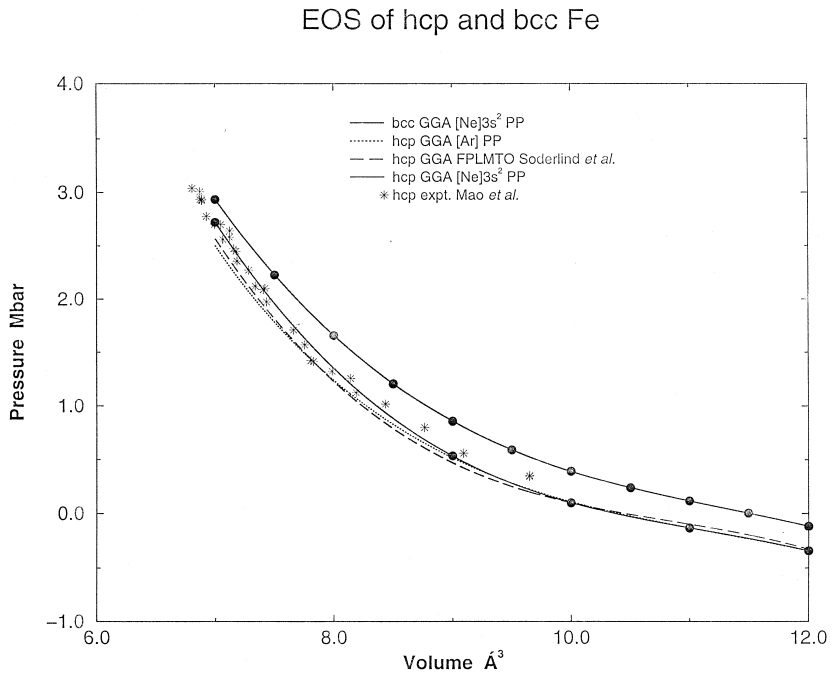

Fig. 2. The equation of state of bcc and hcp iron; the pseudopotential method shows very good agreement with both theory (Södelind et al., 1996) and experiment (Mao et al., 1990).

GPa compared to the experimental value of 10–15 GPa).

2.2. Calculating free energies

The most stable structure of any material at a given P and T is the one with the lowest Gibbs free energy, G, given by:

$$G = U + PV - TS = F + PV$$

where U is the internal energy, V is the volume, S is the entropy and F is the Helmholtz free energy.

Our aim is to calculate $G(P,T)$. In order to do this, we start by calculating the Helmholtz free energy of the crystal as a function of both V and, as discussed below, T. This may be written:

$$F_{\text{total}}(V,T) = F_{\text{perfect}}(V,T) + F_{\text{vibrational}}(V,T)$$

where F_{perfect} is the energy of the rigid perfect lattice, and $F_{\text{vibrational}}$ is the free energy due to atomic vibrations. At zero temperature, F_{perfect} is the total energy of the perfect lattice, U_0, but at high T, it also contains a contribution to the free energy from electronic excitations:

$$F_{\text{perfect}}(V,T) = U_0(V) + U_{\text{el}}(V,T) - TS_{\text{el}}(V,T)$$

In DFT, this contribution is calculated by minimising the Mermin functional in the Kohn–Sham formalism (see, for example de Wijs et al., 1998a,b).

Within the harmonic approximation, the vibrational component of the free energy, including the zero point energy, is obtained from the calculated phonon frequencies, ω_i, via the standard statistical thermodynamics formula:

$$F_{\text{vibrational}}(V,T) = k_{\text{B}}T\sum_i \left(\frac{h\omega_i}{2k_{\text{B}}T} + \ln\left(1 - \mathrm{e}^{\frac{h\omega_i}{k_{\text{B}}T}}\right)\right)$$

Finally, the pressure term in the free energy is obtained from the volume dependence of F using the relation:

$$P = -\left(\frac{\partial F}{\partial V}\right)_T$$

where P has a contribution from the external pressure, P_{ext}, and the thermal pressure, P_{th}:

$$P(V,T) = P_{ext} + P_{th}$$

The Gibbs free energy, $G(V,T)$, may then be obtained from F, P and V.

To calculate the vibrational frequencies, we used the frozen phonon technique, whereby atoms are fixed in positions which are slightly displaced from their perfect equilibrium lattice sites (by $\sim 1\%$), and the resulting forces on all the atoms are calculated. The number and direction of these displacements is governed by symmetry, and if the displacements are sufficiently small and are assumed to be harmonic, the forces are proportional to the displacements; a force-constant matrix may then be constructed, and the phonon frequencies obtained by standard lattice dynamics calculations (e.g., Born and Huang, 1954).

We have calculated this ab initio force constant matrix at three densities representative of the inner core: 13.00, 13.44 and 13.64 g cm^{-3}. We used supercells containing 16 or 32 atoms (the current limit of available resources), with an electronic k-points sampling grid of 6 to 48 k-points in the irreducible Brillouin zone, and with planewave cutoffs chosen to give a convergence in the energy difference between iron phases of better than 0.004 eV/atom. Such high convergence criteria are necessary since the energy difference between the structurally similar phases at core conditions is very small ($\sim$ 0.05–0.01 eV atom).

The phonon frequencies were calculated explicitly at the gamma points, zone boundaries and a mid point position, with interpolation of the dynamical matrix throughout a $19 \times 19 \times 19$ grid; the dispersion curves of each phase were obtained by interpolation along specific symmetry directions. We have assessed the effect of supercell size on the calculated phonon frequencies, and find that this is both systematic and small ($< 0.3\%$ between 16 and 32 atoms of hcp-Fe). Therefore, the influence of supercell size on the free energy *difference* between the polymorphs is very likely to be negligible.

The Gibbs free energy, $G(V,T)$, at each volume is then obtained from the perfect and vibrational contri-

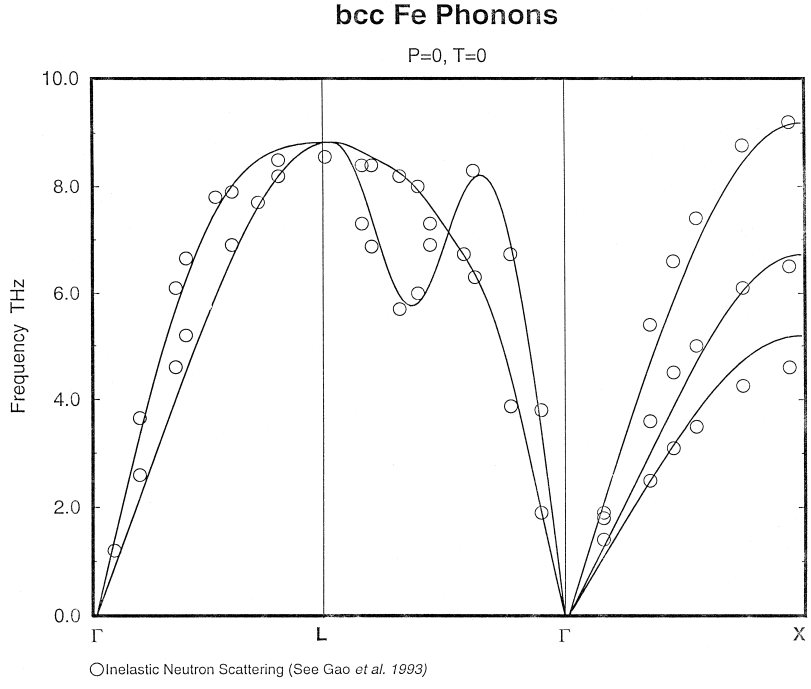

Fig. 3. Calculated phonon dispersion curve for magnetic bcc-Fe under ambient conditions compared with inelastic neutron scattering experiments (open circles).

butions to the Helmholtz free energy ($F_{perfect} + F_{vibrational}$), and the pressure calculated from the thermal and external contributions ($P_{ext} + P_{th}$). As detailed below, analysis of how the total pressure varies as a function of temperature at each volume, in conjunction with how $G(V,T)$ varies as a function

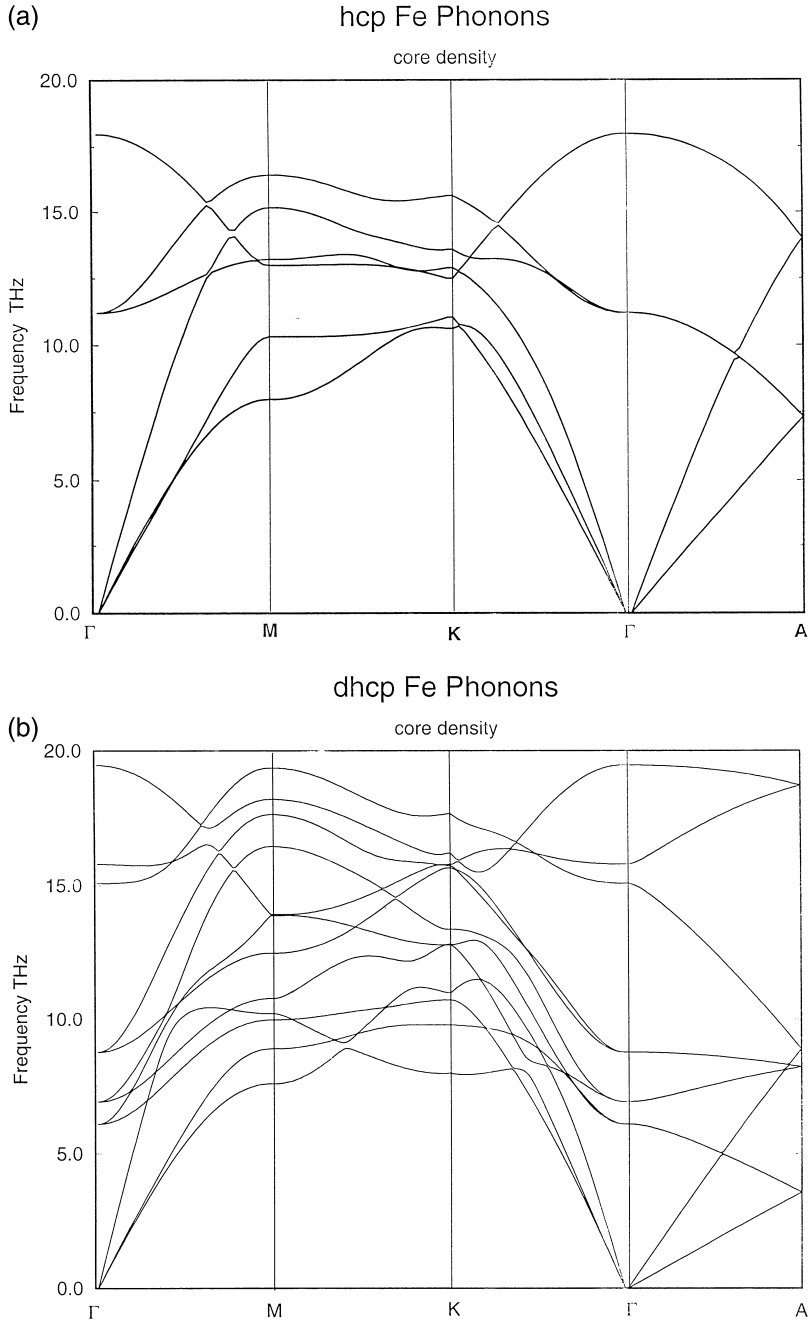

Fig. 4. Calculated vibrational phonon spectrum at core densities of 13 g cm^{-1} for (a) hcp-Fe, (b) dhcp-Fe and (c) fcc-Fe.

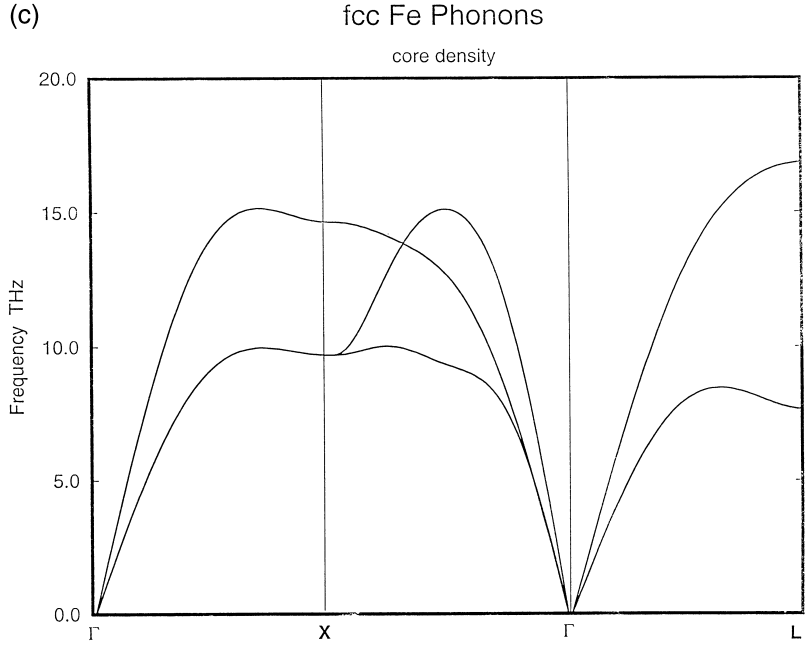

Fig. 4 (continued).

of temperature, allows the construction of $G(P,T)$ along isobars at pressures spanning those thought to exist in the inner core.

3. Results

3.1. Mechanical stability

Fully spin-polarised calculations were performed on all the candidate phases at core pressures (which range from $\sim$325 to 360 GPa). These revealed, in agreement with Södelind et al. (1996), that under these conditions bcc and body-centred tetragonal (bct)-Fe had only a small magnetic moment ($\sim 1/2$ μ_B/atom) and all other phases had zero magnetic moment. We found that at these pressures, the bcc, bct and the recently suggested orthorhombic polymorph of iron (Andrault et al., 1997) are mechanically unstable. The bcc and bct phases continuously transform to the more stable fcc phase with increasing c/a ratio, confirming the findings of Stixrude and Cohen (1995); indeed, Stixrude et al. (1998) suggest the bct phase is *only* stable in a local minimum as a function of c/a geometry, and therefore, never a viable stable structure of iron. The experimentally observed orthorhombic phase spontaneously transforms to the hcp phase when allowed to relax to a state of isotropic stress. In contrast, hcp-, dhcp- (space group $P6_3/mmc$) and fcc-Fe remain mechanically stable at core pressures with c/a ratios of 1.600 for hcp- and 3.207 for dhcp-Fe; we were therefore, able to calculate their phonon frequencies and free energies.

3.2. Thermodynamic stability

In order to assess the quality of our frozen phonon methodology, we first calculated the phonon dispersion curve for fully spin-polarised bcc-Fe at ambient pressure and compared the results with inelastic neutron scattering experiments (see Gao et al., 1993). Our calculated phonon spectrum is in excellent agreement with the experimental data (Fig. 3), therefore supporting the accuracy of our methodology. We then went on to calculate the phonon spectrum for the remaining mechanically stable phases at core conditions (i.e., at a density of 13 g cm^{-3}). Our predicted phonon spectra for fcc-, hcp-, and dhcp-Fe are shown in Fig. 4a,b and c.

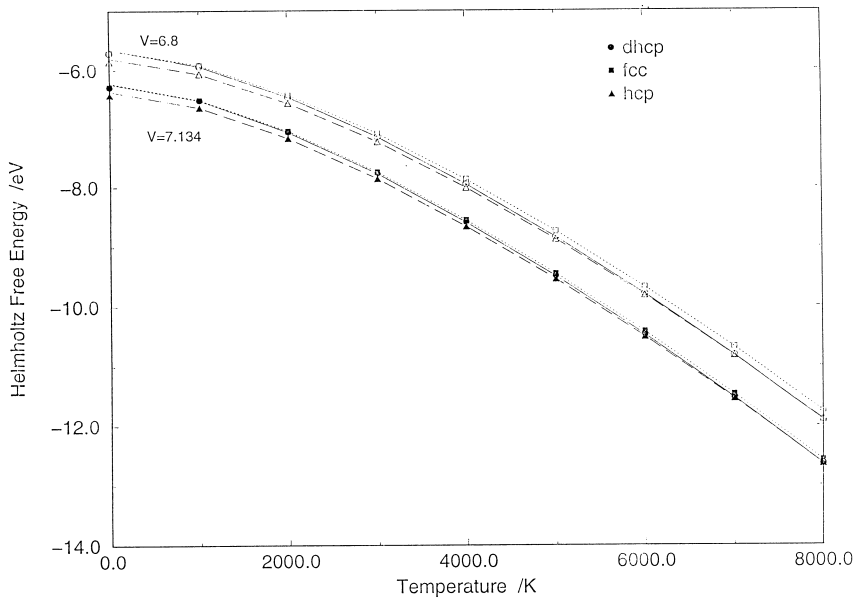

Fig. 5. Calculated temperature dependence of the Helmholtz free energy as a function of temperature at $V = 7.134$ Å^3 (lower curve) and $V = 6.8$ Å^3 (upper curve).

From the calculated phonon frequencies, we may now calculate free energies as a function of temperature. The temperature dependence of the Helmholtz free energy and the thermal pressure (i.e., $P_{\text{total}}(V,T) - P_{\text{perfect}}(V,T=0)$) are shown in Figs. 5 and 6. The thermal pressure at core conditions has been esti-

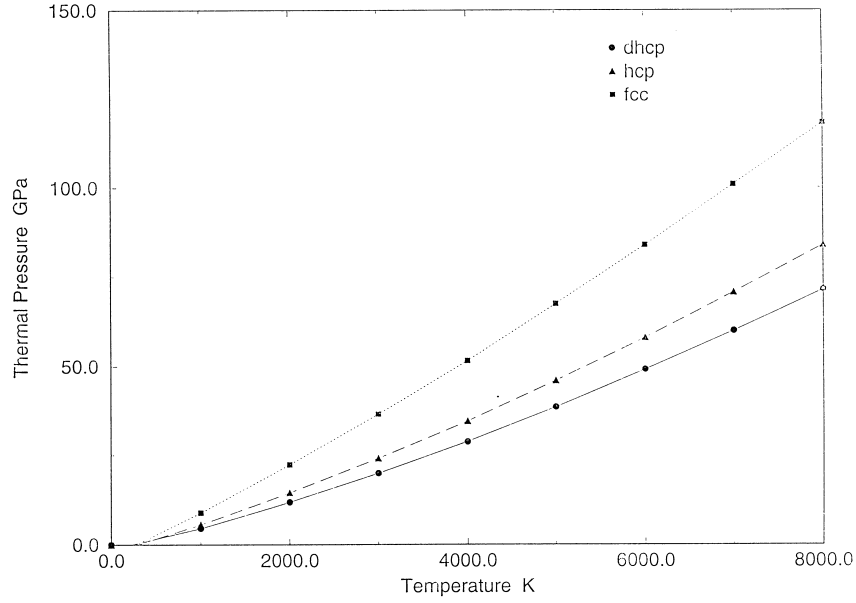

Fig. 6. Calculated thermal pressure as a function of temperature; fcc-Fe is thermodynamically destabilised with respect to the other two phases due to its relatively high thermal pressure.

mated to be 58 GPa (Anderson, 1995) and ≥ 50 GPa (Stixrude et al., 1997); this is in excellent agreement with our calculated thermal pressure for the hcp and dhcp structures (58 and 49 GPa, respectively at 6000 K). However, the calculated thermal pressure is considerably higher for fcc-Fe; this makes the PV term in the Gibbs free energy for this phase very large (3.0 eV at 6000 K compared to 2.2 and 2.5 eV for dhcp and hcp, respectively) and we find that this, therefore, thermodynamically destabilises fcc-Fe at core conditions with respect to dhcp and hcp-Fe.

This far, we have calculated $G(V,T)$ but in order to make any predictions about the relative stability of hcp- and dhcp-Fe at core conditions, $G(P,T)$ is required. An indication that these two phases are going to have very similar free energies is evidenced from their vibrational density of states (Fig. 7), where it can be seen that the vibrational structure is very similar for these two polymorphs which differ only in their third neighbour packing sequence. In order to obtain $G(P,T)$ we proceed as follows: we have P as a function of T for both phases at three separate volumes (Fig. 8a and b); by analysing these, we may see at what temperature $P = 325$ GPa and $P = 360$ GPa (spanning inner core pressures). We may then analyse the data for $G(V,T)$ as a function of T (Fig. 9a and b), and obtain the free energy associated with each of the previously obtained temperatures. These, therefore, must be the free energies at $P = 325$ GPa and $P = 360$ GPa for each of three volumes for both phases; i.e., we have $G(P,T)$ along two isobars (Fig. 10a). An additional constraint on the free energy curve may be obtained from the calculated value for $G(P,T = 0)$. The free energy curves were fitted to an exponential function satisfying the entropic requirement that $(\partial G/\partial T)_{T=0} = 0$ and $(\partial G/\partial T)_{T=0} = (S_{\text{total}})_{\text{calculated}}$. Over the whole P–T space investigated, hcp-Fe has the lower free energy (Fig. 10b and c); therefore, we predict that the stable structure of iron at core conditions is hcp-Fe.

3.3. Thermoelastic properties

From our calculations on hcp-Fe of P as a function of T (Fig. 7a), we were able to obtain a value for the incompressibility, K_T, of this phase at core conditions via the relation:

$$K_T = -\bar{V}\left(\frac{\Delta P}{\Delta V}\right)$$

At core temperatures, this yields a value for K_T at an average density of 13.22 g cm^{-3} of 1356.3 GPa.

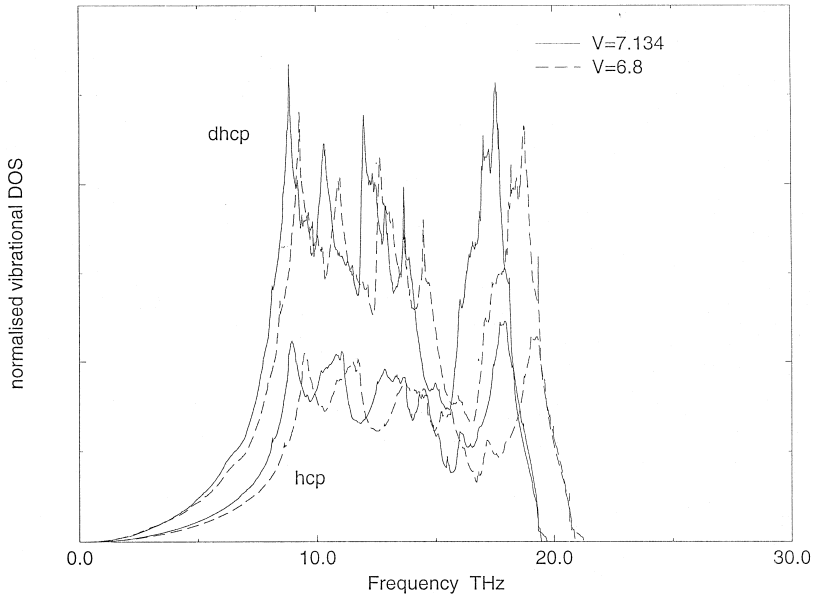

Fig. 7. Calculated vibrational density of states for the hcp and dhcp-Fe which illustrate the structural similarity between these two polymorphs.

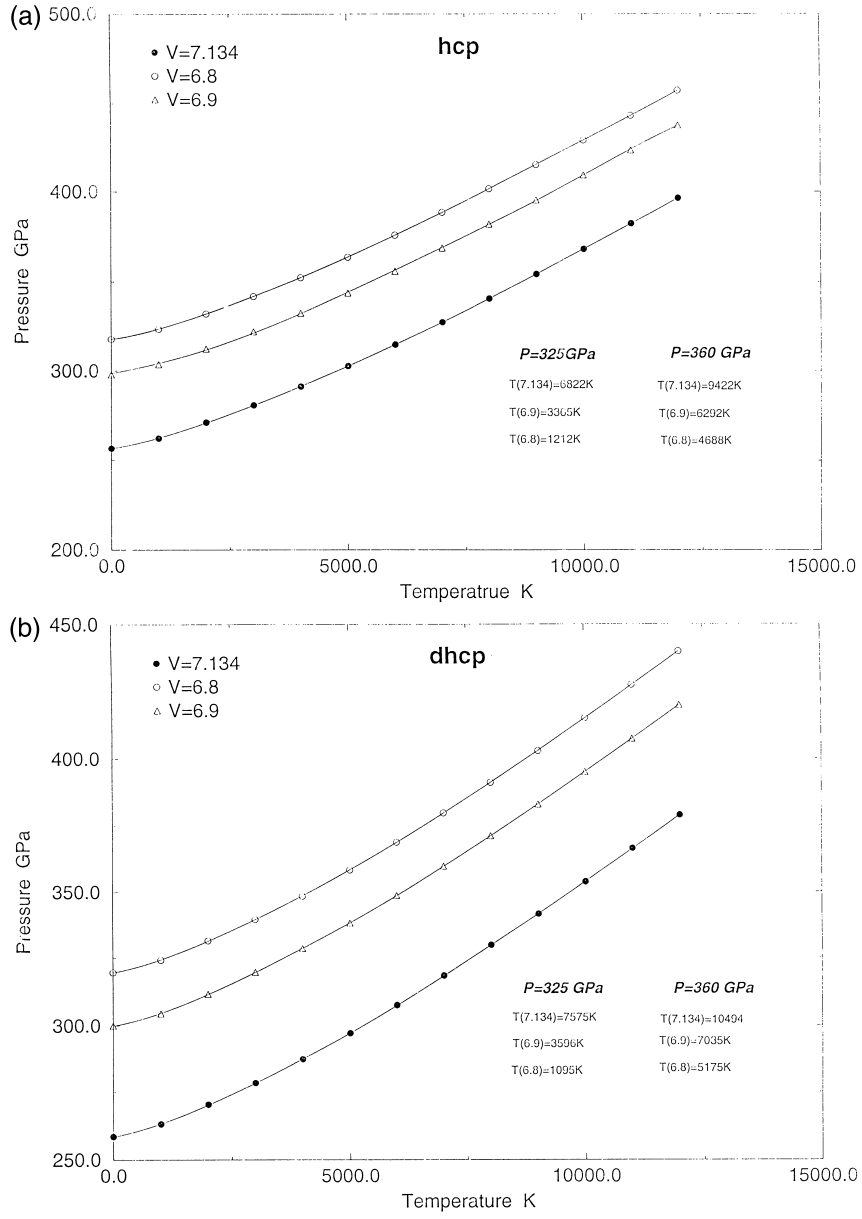

Fig. 8. Total pressure as a function of temperature for (a) hcp-Fe and (b) dhcp-Fe at each of the three volumes, 7.134, 6.9 and 6.8 Å^3. Using this figure, we can see the temperature for which $P = 325$ and 360 GPa for each structure.

We are also able to determine the thermal expansion coefficient, α, at constant pressure from Fig. 10a and the relation:

$$\alpha = \frac{1}{\bar{V}} \frac{\Delta V}{\Delta T}$$

and this gives a value at $\sim$5–6000 K and 325 GPa of $\sim 0.96 \times 10^{-5}$ K^{-1}, in excellent agreement with the values inferred from both shock experiments (Duffy and Ahrens, 1993) and thermoelasticity calculations (Wasserman et al., 1996) of $\sim 0.9 \times 10^{-5}$ K^{-1}.

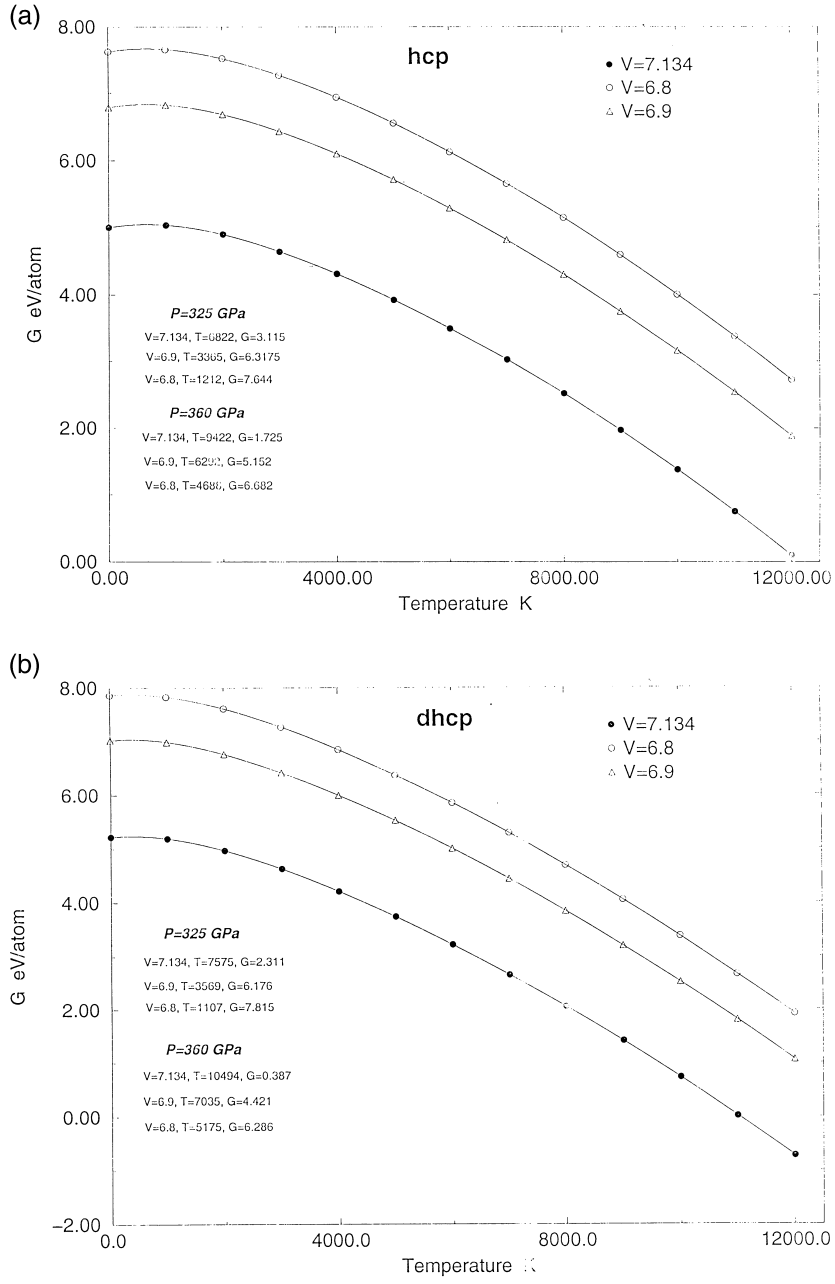

Fig. 9. Gibbs free energy at constant volume as a function of temperature, $G(V,T)$. From this figure, we can obtain $G(P,T)$ along the isobars of 325 and 360 GPa.

A value for the Grüneisen parameter may be obtained from:

$$\gamma = \frac{P_{\text{th}} V}{E_{\text{th}}}$$

where E_{th} is the thermal contribution to the internal energy. This gives a value for γ of 1.7 at 6000 K, in good agreement with the calculations of Wasserman et al. (1996) who obtain $\gamma = 1.6$–1.7 between 1000 and 3000 K at core pressures, and with the high

temperature acoustic γ determined for the inner core of 1.5 (see Anderson, 1995).

From $K_S = K_T(1 + \gamma\alpha T)$, we obtain a K_S of 1489 GPa, and a Φ $(= K_S/\rho)$ of 114 km^2 s^{-2}. This

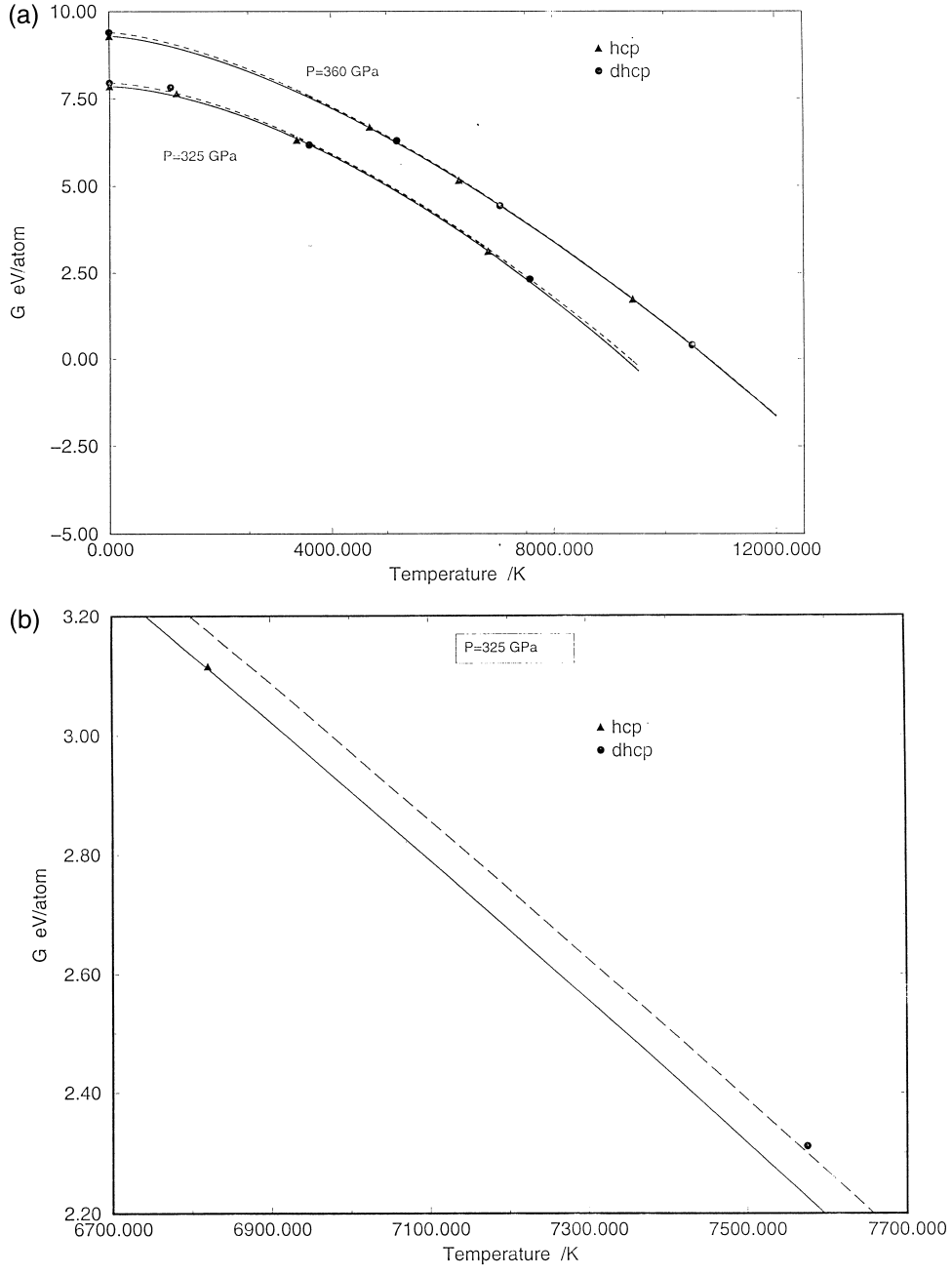

Fig. 10. Calculated Gibbs free energy for hcp-Fe and dhcp-Fe as a function of temperature at $P = 325$ GPa (lower curves) and $P = 360$ GPa (upper curves); hcp-Fe is more stable throughout the whole P/T space shown, as illustrated in the magnifications of the $P = 325$ GPa curves via (b) and (c).

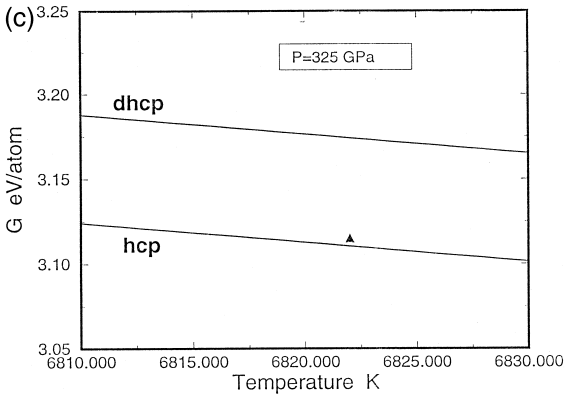

Fig. 10. (continued).

compares well with the PREM value of $105 - 8$ km^2 s^{-2} for the inner core, which contains lighter elements and which would therefore be expected to have a slightly lower value for the seismic parameter than that for the pure iron system calculated here.

4. Discussion

The free energy differences between the hcp and dhcp phases is very small as we would expect for two structures that are so similar. At $P = 325$ GPa, we calculate a ΔG, which is never less than ~ 0.05 eV/atom throughout the whole temperature range. At $P = 360$ GPa, we calculate a ΔG which ranges from ~ 0.05 eV/atom at 4000 K to ~ 0.01 eV/atom at 8000 K. Although these differences are small, they are within the precision of our calculations discussed earlier (< 0.004 eV/atom).

One source of imprecision could be the use of fixed electronic temperature in our calculations. It is possible that there will be a thermal contribution to the electron density and resulting interatomic forces due to electronic excitations, which will affect the phonon frequencies. However, although it is relatively straightforward to calculate F_{perfect} as a function of electronic temperature, it is impracticable to calculate phonon frequencies of large supercells as a detailed function of electronic temperature. Therefore, the supercell calculations were all performed with an electronic temperature of 6000 K, which we consider to be representative of the possible range of temperatures to be found in the inner core. To ensure that the use of fixed electronic temperature did not affect the result, we performed fixed electronic temperature calculations in the expected range of core temperatures (between 4000 and 8000 K). By analysing the ΔF_{total} between dhcp and hcp-Fe, we found that the effect of electronic temperature on free energy is generally significantly smaller than the free energy differences between the phases. ΔF_{total} varied by a maximum of 16% between 4000 and 7000 K, which remains within the precision of the calculation; only at the highest pressure (360 GPa) and temperatures (~ 8000 K) did the difference in ΔF_{total} between dhcp and hcp-Fe become comparable in magnitude with ΔF_{total} itself.

As indicated above, these calculations do not take into account possible anharmonic effects. Over much of the (P,T) range investigated, we believe that we are justified in assuming that the motion of the atoms can be treated as harmonic vibrations, and that all thermodynamic properties can reasonably be calculated from the energy of the static perfect crystal and the harmonic lattice vibrational frequencies (Matsui et al., 1994). This assumption is validated by our calculated thermal expansion coefficient for hcp-Fe discussed earlier, which was in excellent agreement with the values inferred from shock experiments (Duffy and Ahrens, 1993) and thermoelasticity calculations (Wasserman et al., 1996). At the highest temperatures, however, anharmonic effects may become significant, but given the structural similarity of hcp and dhcp-Fe, we would expect anharmonic effects on both phases to be comparable and we suggest that they would have a small, or even negligible, effect on the relative stability of these two polymorphs.

Finally, it has been suggested (Matsui and Anderson, 1997) that although not mechanically stable at zero Kelvin, the bcc phase could be entropically stabilised at high T in the inner core, since bcc retains some magnetic moment at core pressures (Södelind et al., 1996), and it is therefore conceivable that magnetic entropy effects may be non-negligible. However, Moroni and Jarlborg (1996) have estimated that the maximum contribution of magnetic entropy at core conditions is of the order of 0.3 R per mole at 6000 K. The maximum likely contribution to vibrational entropy is comparable to the melting entropy (Stixrude et al., 1994), which

tends to $R\ln 2$ for close-packed metals at high pressures (see Poirier, 1991). Therefore, the total *maximum* entropic contribution is $\sim R$. We calculate that the metastable enthalpy difference between bcc-Fe and hcp-Fe at a density of 13 g/cm^3 is ~ 1.1 eV. For this lattice energy difference to be over come, the entropy difference between the phases would need to exceed $\sim 2R$, and it is therefore improbable that the magnetic and vibrational entropy could overcome this at core conditions.

In conclusion, therefore, our calculations, combined with other evidence, indicate that hcp is the thermodynamically most stable phase of Fe at the conditions believed to exist in the Earth's inner core. Furthermore, from our calculated free energies (Fig. 10a), it can be seen that the free energy difference between the phases *increases* as the temperature decreases, and *increases* as the pressure decreases. This implies that ΔG between the phases would increase significantly as P and T approached the experimentally determined part of the iron phase diagram. Therefore, hcp-Fe would be even more stable with respect to dhcp-Fe at lower P and T. This is in direct conflict with the experimentally determined solid–solid phase transition above 35 GPa (Saxena et al., 1996), yet in agreement with the more recent experiments of Shen et al. (1998). However, fully ab initio molecular dynamics calculations are required that sample the entire P–T space of the iron phase diagram in order to definitively resolve this issue.

Finally, there remains some possibility that an as yet undiscovered phase of iron may exist at inner core conditions; ideally constant stress ab initio molecular dynamics could resolve this issue, but such a calculation is beyond the scope of this paper.

This work provides the basis of further study in which we will determine the effect of anharmonicity on the stability of the iron polymorphs, and establish the equations of state and thermodynamic stability of the iron alloys thought to exist in the inner core.

References

Anderson, O.L., 1995. Equations of State of Solids for Geophysics and Ceramic Science. Oxford Monographs on Geology and Geophysics, 31. Oxford Univ. Press, Oxford.

Anderson, O.L., Duba, A., 1997. Experimental melting curve of iron revisited. J. Geophys. Res. 102, 22659–22669.

Andrault, D., Fiquet, G., Kunz, M., Visocekas, F., Häusermann, D., 1997. The orthorhombic structure of iron: an in situ study at high temperature and high pressure. Science 278, 831–834.

Bassett, W.A., Weathers, M.S., 1990. Stability of the body-centred cubic phase of iron — a thermodynamic analysis. J. Geophys. Res. 95, 21709–21711.

Boehler, R., 1993. Temperature in the Earth's core from the melting point measurements of iron at high static pressures. Nature 363, 534–536.

Born, M., Huang, K., 1954. Dynamical Theory of Crystal Lattices. Oxford Univ. Press, Oxford, UK.

Brown, J.M., McQueen, R.G., 1986. Phase transitions, Grüneisen parameter and elasticity for shocked iron between 77 GPa and 400 GPa. J. Geophys. Res. 91, 7485–7494.

de Wijs, G.A., Kresse, G., Gillan, M.J., 1998a. First order phase transitions by first principles free energy calculations: the melting of Al. Phys. Rev. B 57, 8223–8234.

de Wijs, G.A., Kresse, G., Vočadlo, L., Dobson, D., Alfe, D., Gillan, M.J., Price, G.D., 1998b. The viscosity of liquid iron at the physical conditions of the Earth's core. Nature 392, 805–807.

Duffy, T.S., Ahrens, T.J., 1993. Thermal expansion of mantle and core materials at very high pressures. Geophys. Res. Lett. 20, 1103–1106.

Gao, F., Johnston, R.L., Murrell, J.N., 1993. Empirical many-body potential energy functions for iron. J. Phys. Chem. 97, 12073–12082.

Kresse, G., Furthmüller, J., 1996. Efficient iterative schemes for ab initio total energy calculations using planewave basis set. Phys. Rev. B 54, 11169–11186.

Kresse, G., Hafner, J., 1994. Normconserving and ultrasoft pseudopotentials for first row elements and transition metals. J. Phys.: Condens. Matter 6, 8245–8257.

Mao, H.K., Wu, Y., Chen, L.C., Shu, J.F., Jephcoat, A.P., 1990. Static compressions of iron to 300 GPa and $Fe_{0.8}Ni_{0.2}$ alloy to 260 GPa — implications for the composition of the core. J. Geophys. Res. 95, 21737–21742.

Matsui, M., Molecular dynamics study of iron at Earth's inner core conditions. AIP Conference Proceedings, American Institute of Physics, 1993, pp. 887–891.

Matsui, M., Anderson, O.L., 1997. The case for a body-centred cubic phase (α') for iron at inner core conditions. Phys. Earth Planet. Inter. 103, 55–62.

Matsui, M., Price, G.P., Patel, A., 1994. Comparison between the lattice dynamics and molecular dynamics methods: calculation results for $MgSiO_3$ perovskite. Geophys. Res. Lett. 21, 1659–1662.

Moroni, E.G., Jarlborg, T., 1996. Bcc and hcp phase competition in Fe. Europhys. Lett. 33, 223–228.

Moroni, E.G., Kresse, G., Furthmüller, J., Hafner, J., 1997. Pseudopotentials applied to magnetic Fe, Co and Ni: from atoms to solids. Phys. Rev. B 56, 15629–15646.

Nguyen, J.H., Holmes, N.C., 1998. Iron sound velocities in shock wave experiments up to 400 GPa. AGU Abstracts, 79, T21D-06.

Perdew, J.P., Chervary, J.A., Voska, S.H., Jackson, K.A., Perderson, M.R., Singh, D.J., Fiolhais, C., 1992. Atoms, molecules, solids and surfaces — applications of the generalised gradient approximation for exchange and correlation. Phys. Rev. B 46, 6671–6687.

Poirier, J.P., 1991. Introduction to the Physics of the Earth's Interior. Cambridge Univ. Press.

Saxena, S.K., Dubrovinsky, L.S., Häggkvist, P., 1996. X-ray evidence for the new phase of β-iron at high temperature and high pressure. Geophys. Res. Lett. 23, 2441–2444.

Shen, G.Y., Mao, H.K., Hemley, R.J., Duffy, T.S., Rivers, M.L., 1998. Melting and crystal structure of iron at high pressures and temperatures. Geophys. Res. Lett. 25, 373–376.

Södelind, P., Moriarty, J.A., Wills, J.M., 1996. First principles theory of iron up to Earth core pressures: structural, vibrational and elastic properties. Phys. Rev. B 53, 14063–14072.

Stixrude, L., Cohen, R.E., 1995. Constraints on the crystalline structure of the inner core: mechanical instability of BCC iron at high pressure. Geophys. Res. Lett. 22, 125–128.

Stixrude, L., Cohen, R.E., Singh, D.J., 1994. Iron at high pressure: linearised augmented planewave computations in the generalised gradient approximation. Phys. Rev. B 50, 6442–6445.

Stixrude, L., Wasserman, E., Cohen, R.E., 1997. Composition and temperature of the Earth's inner core. J. Geophys. Res. 102, 24729–24739.

Stixrude, L., Wasserman, E., Cohen, R.E., 1998. First principles investigations of solid iron at high pressure and implications for the Earth's inner core. In: Manghnani, M.H., Yagi, T. (Eds.), Properties of the Earth and Planetary Materials at High Pressures and Temperature. AGU, pp. 159–171.

Vanderbilt, D., 1990. Soft self-consistent pseudopotentials in a generalised eigenvalue formalism. Phys. Rev. B 41, 7892–7895.

Vočadlo, L., de Wijs, G., Kresse, G., Gillan, M., Price, G.D., 1997. First principles calculations on crystalline and liquid iron at Earth's core conditions. Faraday Discuss. 106, 205–217.

Wasserman, E., Stixrude, L., Cohen, R.E., 1996. Thermal properties of iron at high pressures and temperatures. Phys. Rev. B. 53, 8296–8309.